Available online at www.sciencedirect.com
SCIENCE DIRECT
Cement & Concrete Composites 28 (2006) 237–245
Cement & Concrete Composites
www.elsevier.com/locate/cemconcomp

Study of the chloride diffusion in mortar: A new method of determining diffusion coefficients based on impedance measurements

B. Díaz, X.R. Nóvoa *, M.C. Pérez

Universidade de Vigo, ETSEI, Campus Universitario, 36310 Vigo, Spain

Available online 14 February 2006

Abstract

Chloride diffusion coefficients can be obtained from traditional two-compartment cell experiments. Typically, either natural diffusion or migration methods are employed. These conventional tests are time-consuming and laborious; thus, in order to obtain chloride diffusion coefficients in shorter time periods, we propose a new method based in impedance spectroscopy. Impedance measurements in the 40 MHz to 100 Hz frequency range allow to obtain diffusion coefficients that correlate well either with those reported in the literature and those obtained using traditional diffusion and migration tests.

Keywords: Chlorides; Diffusion; Migration; Impedance measurements

1. Introduction

Chloride ions ingress is a common cause of deterioration of reinforced concrete structures since chlorides can initiate corrosion of the reinforcement which, by expansion pressure, cracks the concrete cover. Concrete may be exposed to chlorides by seawater contact or deicing salts. The ability of chloride ions to penetrate the concrete must then be known for estimating structure's durability.

The penetration of chloride ions into concrete is a relatively slow process, which forces the development of testing methods able to supply diffusion coefficient values in a reasonable time scale.

Conventional measurement techniques involve the preparation of permeation cells in which the tested sample acts as membrane between two solutions, one of them highly concentrated in chloride and the other one diluted or even distilled water. Fig. 1 shows schematically the arrangement. Chlorides will traverse the membrane from the concentrated solution to the diluted one either acting the concentration gradient as driving force (natural diffusion) or under the action of an electric field (migration).

Diffusion coefficients calculations are performed on the basis of the rate of concentration change in the diluted compartment (or down stream compartment) of the permeation cell (see Fig. 1). According to the literature [1], most experimental methods used are based on electrical techniques because testing time is reduced by two orders of magnitude. Natural diffusion tests take about 100 days to be completed while migration tests (under applied DC field) take only several hours. Nevertheless, these accelerated experiments present important disadvantages which will be analysed afterwards.

The ASTM C1202 (AASHTO T277) is a rapid chloride permeability test in which a water-saturated sample is exposed to 60 V DC for 6 h and the total charge passed is determined. The chloride penetrability is proportional to the charge passed. Although this test is widely used, it is criticized because: the measured charge corresponds to the movement of all ions present in pore solution (not just chloride ions), the high voltage causes an increase in temperature, and the results give only qualitative information, no diffusion coefficient values can be obtained.

Other methods using lower intensity electric field are often used to accelerate the chlorides movement. Those methods (electrochemical migration techniques) have been extensively analysed by Andrade [2]. The movement of ions

* Corresponding author. Tel./fax: +34986812213.
E-mail address: rnovoa@uvigo.es (X.R. Nóvoa).

0958-9465/$ - see front matter © 2006 Elsevier Ltd. All rights reserved.
doi:10.1016/j.cemconcomp.2006.01.009

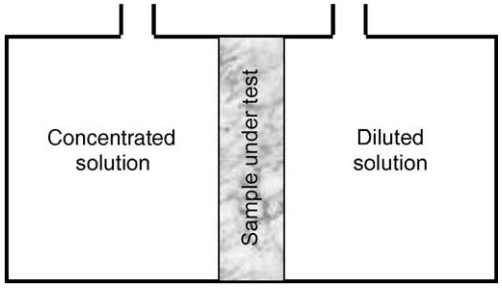

Fig. 1. Typical two-compartment cell (permeation cell) employed in diffusion and migration tests (schematic).

in solution under electric field is governed by the Nernst–Planck equation:

$$-J_i = D_i \frac{\delta C_i(x)}{\delta x} + \frac{zF}{RT} D_i C_i \frac{\delta E(x)}{\delta x} - C_i v_i(x) \quad (1)$$

where J_i is the flux of the ionic species i, D_i is the diffusion coefficient of i, $C_i(x)$ is the concentration of i as a function of x, z_i is the ionic valence, F is Faraday's constant, R is the universal gas constant, T is temperature, $E(x)$ is the applied electric potential and v_i is the velocity of i.

Considering the situation where there is no convection and assuming that pure diffusion is negligible compared to the effect of electrical migration, and that the electric field is linear through the sample of thickness ℓ, Eq. (2) is obtained from Eq. (1):

$$J_i = \frac{zFD_iC_iE}{RT\ell} \quad (2)$$

Eq. (2) allows the calculation of D_i by determining J_i as concentration variation with time. It is assumed that C_i is constant in the cathodic side and steady state conditions have been reached.

Although migration tests are used by many authors, they are though to be unrealistic since they do not take into account the mortar damage generated at the mortar-anodic solution interface, aspect that will be illustrated later.

The various theoretical and practical problems inherent to the above discussed tests justify the search for an alternative method of diffusion coefficient determination. This paper presents a new approach based on impedance spectroscopy (IS), which overcomes those problems.

In the last decade IS technique in high frequency region has been presented as a suitable method to characterize microstructure of cementitious materials and to study their electrical properties [3–6]. In this paper, a relationship will be established between electrical properties and chloride diffusion coefficient.

2. Experimental

2.1. Specimens

Mortar samples were prepared using Portland cement type CEM I 52.5 R according to UNE 80 301:96 standard, with water/cement and cement/sand ratios of 0.45 and 1/3, respectively. The mixtures were cast in moulds of $16 \times 4 \times 16$ cm and cured at 100% RH chamber during 24 h. Afterwards the samples were demoulded and maintained in the chamber up to more than 28 days curing, before starting the measurements. Samples for experiments were cut to 4 cm thick.

2.2. Testing cell

An example of the permeation cells employed is depicted in Fig. 2. One of the compartments is filled with sodium chloride solution while the other encloses sodium hydroxide solution. Solutions employed in migration tests were NaOH 0.3 M in anodic side and NaCl 0.5 M in the cathodic side (according to ASTM C1202). For impedance measurements the solutions were NaOH 0.01 M and NaCl 0.5 M or 1 M with NaOH 0.01 M, if not otherwise specified. The volume of each compartment is 200 cm^3. Four o-ring define 20 cm^2 wetted surface at both ends of the cell (where graphite sheets are located) and at both sides of the mortar membrane.

2.3. Measuring techniques

Impedance measurements using two electrode arrangement (between graphite sheets in Fig. 2) were performed using a HP 4194A impedance/gain-phase analyser which measures impedance from 40 MHz down to 100 Hz in pure AC mode (no DC bias needed). The HP 4194A measures capacitance in the 10^{-14}–10^{-1} F range with maximum resolution of 10^{-15} F.

Four electrodes impedance measurements were performed using a potentiostat/galvanostat PGSTAT 30 with FRA module, from Ecochemie. The nominal maximum

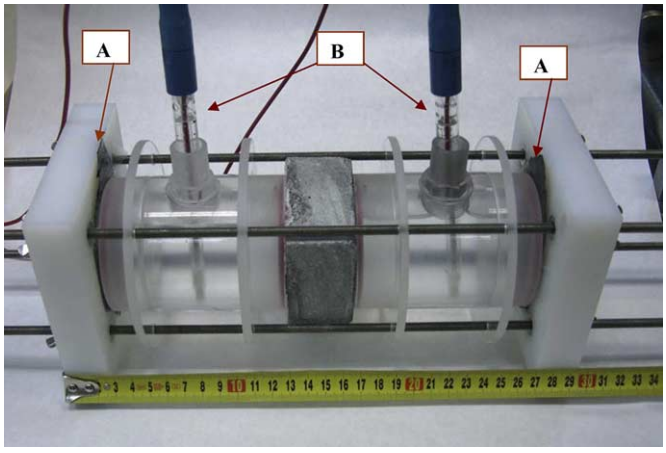

Fig. 2. One of the permeation cell employed in this work. The mortar membranes are 4 cm thick and the o-rings at both sides define 20 cm^2 wetted surface. (A) Graphite sheets for applying the electric field (DC and/or AC). (B) SCE reference electrodes for four electrode impedance measurements. When platinum wires were employed they were located close to the membrane.

frequency is 1 MHz, however, accurate measurements can be obtained only to about 200 kHz. The four electrode arrangement was constituted by two external graphite sheets as counter electrodes, and two internal platinum wires (or, in some cases, saturated calomel electrodes), located close to the sample, acting as sensing electrodes. In the two electrodes arrangement there was only the two external graphite sheets.

The evolution of chloride concentrations was followed using a Metrohm chloride-selective electrode for measuring chloride concentration.

Changes in mortar's microstructure were evaluated using mercury intrusion porosimetry (MIP) measurements in an Autopore IV 9500 from Micromeritics. The covered pores diameter range is from 18 μm down to 5 nm.

A Crison model Basic 20 pH meter was employed for pH determinations in the anodic and cathodic compartments.

3. Results and discussion

3.1. Concerns about migration tests

According to literature [1,7] 12 V DC is a good choice for conducting migration tests because chloride transport is accelerated and heat dissipated is not high enough to increase sample's temperature. Thus, a first set of experiments was planned with the aim of highlight possible problems concerning these tests.

Table 1 summarises the chloride flux from the cathodic to the anodic compartment. The flux was obtained by measuring the concentration changes in both compartments. It can be seen that after 100 h inward flux to sample is still higher than chloride outward flux. Consequently, steady state conditions have not been reached along the migration test and therefore the application of Nernst–Planck equation is not strictly correct.

The reason for the observed difference between inward and outward chloride fluxes is probably due to the reaction between cement and chlorides to form Friedel's salt, as evidenced in Fig. 3.

Electrolysis of water takes place due to the applied electric potential, generating H_2 and O_2 (Eqs. (3) and (4) respectively). Thus, important pH changes shall occur in both compartments.

$$2H_2O + 2e^- \rightarrow H_2 + 2OH^- \quad (3)$$

$$2H_2O \rightarrow O_2 + 4H^+ + 4e^- \quad (4)$$

Table 1
Inward and outward flux and cathodic chloride concentration during the migration test (12 V)

Time (h)	$[Cl^-]_{cathodic}$ (M)	Inward flux (mol cm^{-2} s^{-1})	Outward flux (mol cm^{-2} s^{-1})
0	0.5	–	–
100	0.33	4.93×10^{-9}	4.03×10^{-9}

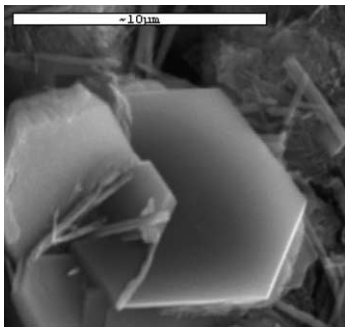

Fig. 3. SEM micrograph showing the hexagonal morphology typical of Friedel's salt. Obtained after 900 h natural diffusion test.

Fig. 4 shows the pH evolution in the anodic and cathodic compartments up to 600 h testing. Important pH changes occur during the first 200 h. It can be seen that pH in the anodic compartment decreases to less than 2. This very low pH damages the sample as it can be seen visually in Fig. 5. The acid attack completely destroys sample's microstructure at the anodic side, as revealed by MIP analysis (Fig. 6(A)). Nevertheless sample's core preserves its original structure, as it can be seen from the comparison of Fig. 6(B) and (C). The only difference concerns the small size pore family (between 1 and 10 nm) which starts

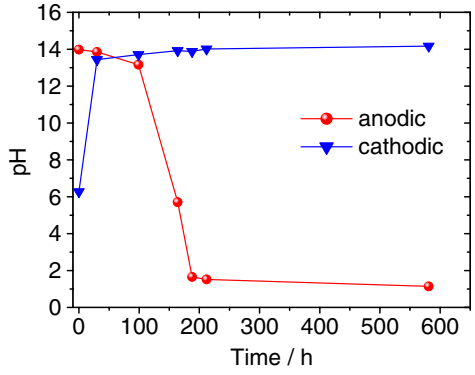

Fig. 4. Evolution of pH values of the anodic and cathodic solutions in migration test. At time = 0 the solutions were 0.3 M NaOH and 0.5 M NaCl, anodic and cathodic compartment, respectively.

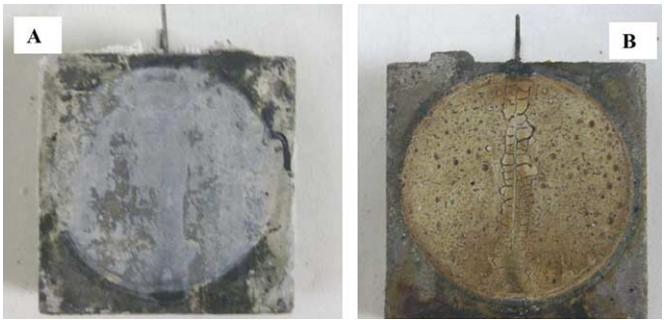

Fig. 5. View of both sides of one of the tested samples after migration test. The sides facing the cathodic compartment (A) and (B) anodic are shown.

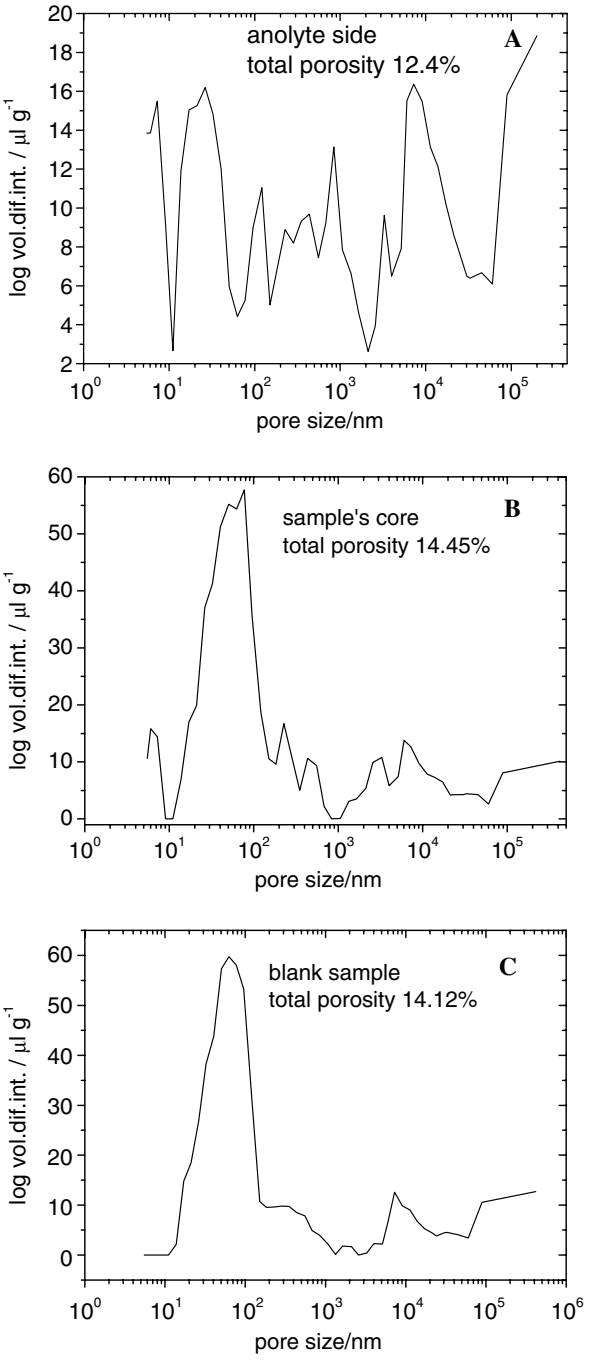

Fig. 6. Mercury intrusion porosimetry results obtained from mortar after migration test, at the anolyte side (A), at the sample's core (B), and from a blank sample (C).

developing in the presence of chlorides. This new pore family is probably related to the aforementioned Friedel's salt formation.

3.2. Four-electrode impedance measurements

The accelerating effect of migration experiment with respect to the standard diffusion experiment was examined by measuring sample's impedance changes over time. Four-electrode impedance measurements were first performed to ensure measurements free of electrode interface contributions.

Impedance measurements should be sensitive enough to detect small structural changes due to chloride-cement reaction and thus the applied DC field was limited to 5 V in order to measure early changes.

The comparison of Fig. 7(A) and (B) shows that sample's impedance increases with testing time, which can be interpreted on the basis of the changes in porosity due to chloride-cement reaction (see Fig. 6(B) and (C) above discussed). Moreover, the applied DC potential accelerates changes inside the samples by about one order of magnitude with respect to natural diffusion test, because the impedance spectra at 70 h (natural test, Fig. 7(A)) and at 7 h (migration test, Fig. 7(B)) are very close. The impedance spectra shown in Fig. 7(A) and (B) can be modelled according to the equivalent circuit reported in the literature and represented in Fig. 7(B). The impedance for this equivalent circuit corresponds to Eq. (5) where R_e accounts for the electrolyte resistance between the sensing electrodes and the mortar sample, C_1 is the dielectric capacitance associated to the solid phase of the mortar, R_1 is related to ionic motion in percolating porosity, and C_2 and R_2

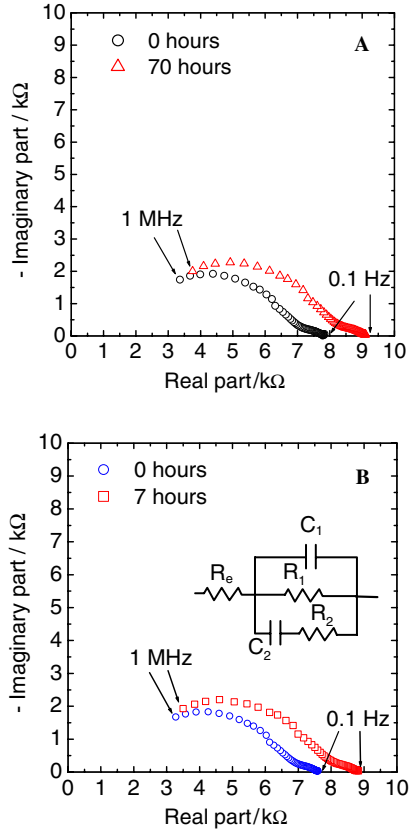

Fig. 7. Four-electrode impedance spectra obtained on mortar samples (4 cm thick, 20 cm^2 wetted surface) using 0.1 M and 0.01 M NaCl solutions: (A) Natural diffusion at $t = 0$ and after 70 h testing. (B) Migration test (5 V DC) at $t = 0$ and after 7 h testing. The equivalent circuit employed to model the data is also depicted (see text).

Table 2
Best fitting parameter values obtained by a simplex method used to fit data in Fig. 7(B) (data at 7 h) to Eq. (5)

R_e (Ω)	C_1 (pF)	R_1 (Ω)	R_2 (Ω)	C_2 (nF)	α_1	α_2
1592	103	7330	29,636	2.1	0.79	0.35

are related to double layer effects and ionic motion in occluded porosity [6,8].

$$Z(\omega) = R_e + \frac{Z_1 \cdot Z_2}{Z_1 + Z_2} \text{ being } Z_1 = \frac{R_1}{1 + (j\omega R_1 C_1)^{\alpha_1}} \text{ and}$$

$$Z_2 = R_2(1 + (j\omega R_2 C_2)^{-\alpha_2}) \quad (5)$$

$$\varepsilon = \frac{C_1 d}{\varepsilon_0 S} \quad (6)$$

The model parameter C_1 allows obtaining the dielectric constant of the sample, ε, through Eq. (6), where d represents sample's thickness (4 cm) and S the active cross section (20 cm^2). ε_0 is the vacuum permittivity (8.85×10^{-14} F cm^{-1}).

The ε value obtained using Eq. (6) and the C_1 value given in Table 2 is 233, which is far from expected for a ceramic material as mortar. Moreover, R_e value is not compatible with the small resistivity of the solutions employed. These facts suggest that the main contribution of the sample's impedance remains out of the measured frequency window.

3.3. Two-electrode versus four-electrode impedance measurements

The two-electrode measurement in permeation cells (Figs. 1 and 2) has the disadvantage that the time constant corresponding to the driven electrodes/electrolyte interface can mask the impedance of the membrane. Nevertheless, the frequency window of the two-electrode measurement is larger in the high frequency limit which will be of major importance in this case.

The comparison of the two- and four-electrode impedance measurements allows to establish the degree of overlapping of the time constants corresponding to the driving electrodes and those corresponding to the membrane. Fig. 8 corresponds to one of these comparisons. The frequency range from 1 MHz to 100 kHz for the four-electrode measurement has been removed because of the associated measurement error inherent to the potentiostat.

The data presented in Fig. 8 confirm the hypothesis advanced in Section 3.2 that most of the contribution of the membrane appears in the frequency range above the four-electrode measurement window. Moreover, the low frequency part of the impedance spectrum is coincident for both types of measurements, which means that the driving electrode's impedance will start to contribute at frequencies below 100 Hz (the low frequency limit of our two-electrode measurement).

As the high frequency part ($f > 10$ kHz) of the impedance spectrum in Fig. 8 corresponds to two time constants,

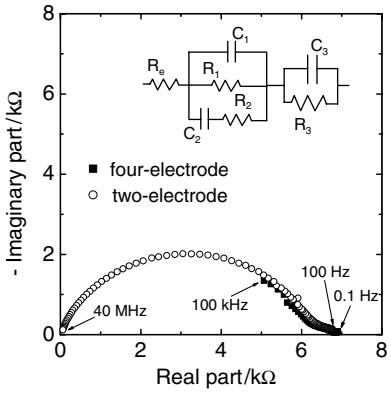

Fig. 8. Impedance measurements on a 4 cm thick mortar sample using two and four electrode arrangement. The measurements were performed after 7 h migration test (5 V DC), using 0.5 M NaCl electrolyte. The equivalent circuit employed to model two-electrode data is also depicted (see text).

it is clear that the capacitive arc present in the low frequency limit belongs to some other contribution and thus the interpretation given in Section 3.2 is erroneous.

The interface mortar/solution, as every interface, shall have resistive and capacitive behaviour that can appear in the impedance spectrum in the form of a low frequency capacitive arc. Thus the full equivalent circuit must include this contribution, represented in Fig. 8 as R_3C_3. The expression of the total impedance of the model is given in Eq. (7).

$$Z(\omega) = R_e + \frac{Z_1 \cdot Z_2}{Z_1 + Z_2} + \frac{R_3}{1 + (j\omega R_3 C_3)^{\alpha_3}} \quad (7)$$

(The expressions for Z_1 and Z_2 are given in Eq. (5).)

The best fitting values of Eq. (7) parameters to the two-electrode measurement data presented in Fig. 8 are summarised in Table 3. Now the R_e value corresponds well to the electrolytes conductivity and from the C_1 value and Eq. (6), a reasonable value of 65 is obtained for the apparent dielectric constant.

3.4. Migration tests and impedance measurements

Migration tests using water saturated samples and 12 V DC were performed, measuring chloride concentrations in the anodic and cathodic compartments. Fig. 9 shows the evolution of chloride concentration in the anodic compartment with time. These values allow obtaining (through Eq. (2)) the diffusion coefficients reported in Table 4.

Table 4 shows that diffusion coefficient decreases as testing time increases, which can be attributed to Friedel's salt formation and microstructural modifications discussed in Section 3.1. Moreover, Table 4 shows also that chloride concentration in the cathodic compartment decreases up to 50% during the migration experiment, which introduces an underestimation error when Eq. (2) is employed to obtain diffusion coefficients. Parallel to the migration experiments, impedance measurements were done between

Table 3
Best fitting parameter values obtained by a simplex method used to fit data in Fig. 8 (two-electrode measurement) to Eq. (7)

R_e (Ω)	C_1 (pF)	R_1 (Ω)	C_2 (pF)	R_2 (Ω)	C_3 (μF)	R_3 (Ω)	α_1	α_2	α_3
114.9	28.6	6188.0	24.14	2320.7	2.5	1217.7	1.0	0.67	0.36

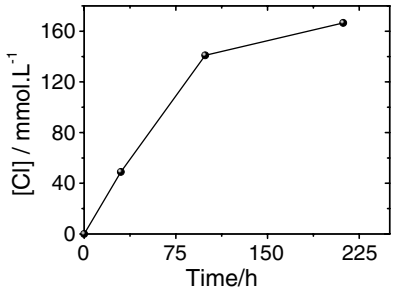

Fig. 9. Chloride concentration in the downstream (anodic) compartment for 12 V DC migration test. Water saturated sample. Mortar with w/c ratio = 0.45.

Table 4
Chloride diffusion coefficients obtained from chloride concentration values represented in Fig. 9, and chloride concentrations in the cathodic compartment

t (h)	D ($cm^2\ s^{-1}$)	$[Cl^-]_{cathodic}$ (M)
30	3.64×10^{-8}	0.5
100	3.17×10^{-8}	0.33
200	1.75×10^{-8}	0.25

the two external graphite sheets. Fig. 10 shows evolution of Nyquist plots with migration test time. It can be seen that the overall impedance increases with time which is in agreement with the above discussed changes in mortar's microstructure and with the observed decreasing in diffusion coefficient (see Table 4). This last aspect will be discussed later in Section 3.5.

The set of impedance data to which those presented in Fig. 10 correspond have been modelled using Eq. (7) (equivalent circuit depicted in Fig. 8). The best fitting parameters are given in Fig. 11(A) and (B). The observed variations are discussed next.

As stated in Section 3.2, R_e is related with the solution resistance (both compartments) and thus remains essentially constant with time. In the present case the anolyte (0.01 M NaOH) presents lower conductivity than the catholyte (0.01 M NaOH + 0.5 M NaCl); therefore, the anolyte contribution to the final resistance value will be dominant. The anolyte conductivity is about 2 mS cm^{-1}, which corresponds to a resistance value of 100 Ω (because the cell constant is 0.2 cm^{-1}). This value is very close to R_e.

The model employed attributes R_1 to the ionic resistance of the sample. It can be seen in Fig. 11(A) that, after the initial decreasing, it increases with time. The initial decreasing can be attributed to filling of still empty percolating pores while subsequent increasing shall be related to the above mentioned Friedel's salt formation which blocks percolating pores, decreasing the number of diffusion paths.

R_2 value decreases during the test, which is agreement with the appearance of Friedel's salt: the number of non-percolating pores increases as percolating porosity decreases (R_1 increases).

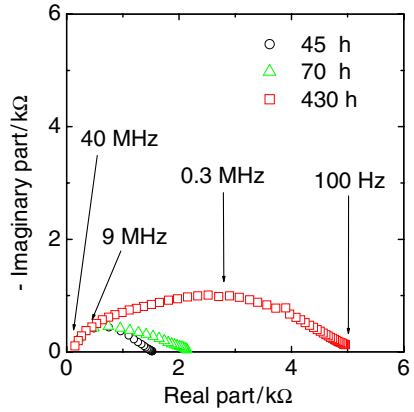

Fig. 10. Two-electrode impedance Nyquist plots obtained at different times during a migration experiment. Electrolytes: 0.01 M NaOH (anolyte) and 0.5 M NaCl + 0.01 M NaOH (catholyte).

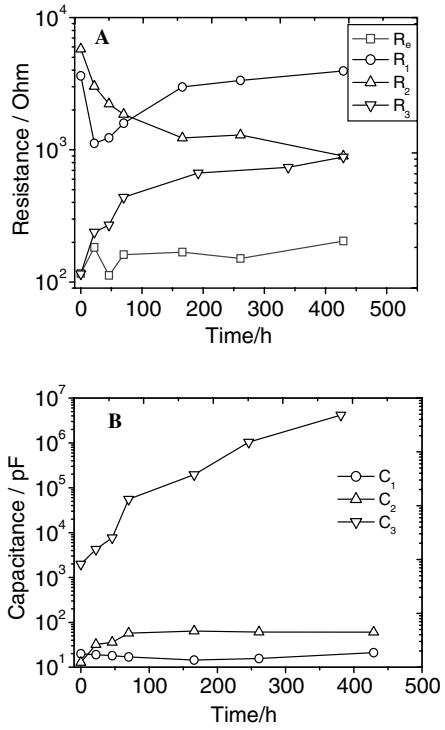

Fig. 11. Best fitting parameters obtained when fitting the impedance spectra given in Fig. 10 (and the remaining spectra not shown therein) to Eq. (7).

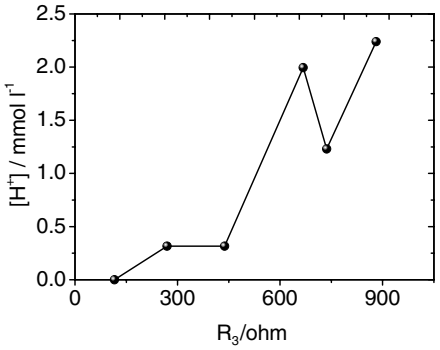

Fig. 12. Relationship between R_3 values and pH in the anodic compartment. R_3 data taken from Fig. 11(A).

The observed increasing of R_3 with time can be interpreted as thickening of the precipitate formed on mortar at the anolyte interface (Fig. 5(B)). In Fig. 12 a relationship between R_3 and H^+ concentration is shown. It can be seen that R_3 increases as $[H^+]$ does (so it is related to the damage on mortar's skin). This fact supports the assignation made in Section 3.3 when the time constant R_3C_3 was assigned to the mortar–solution interface.

Fig. 11(B) shows that C_1 values do not change significantly with testing time indicating that the fraction of solid phase remains essentially constant, which is in agreement with PIM results reported in Fig. 6(B) and (C).

The C_2 increase can be due to the increase of pore surface due to the new pore's family growing below 10 nm (see Fig. 6(B) and (C)). The variation of R_2 and C_2 is coherent with this interpretation.

In Fig. 11(B) and C_3 values are about μF. These values shall correspond to double layer capacitance associated to the powdery nature interface between sample and solution. The powder active surface increases as mortar degradation proceeds.

3.5. Diffusion coefficients from R_1

Chlorides diffusion coefficient, the parameter of interest in structure's lifetime prediction, is directly related to the ionic motion in percolating pores. From the electrical equivalent model point of view this ionic motion is measured R_1. Therefore R_1 can be correlated to the sample's conductivity which in turn allows calculating diffusion coefficient [9].

The resistivity of the sample is obtained directly from R_1 using Eq. (8), where a is sample's cell constant (thickness-to-area ratio), 1/5 in our case.

$$\rho = \frac{R_1}{a} \tag{8}$$

The sample's conductivity (inverse of resistivity) is due to the total ionic mobility, according to Eq. (9):

$$\frac{1}{\rho} = F \sum_j z_j u_j C_j \tag{9}$$

where z_j corresponds to the charge of ion j, C_j is ion concentration (assuming activity coefficient close to 1) and u_j is the ionic mobility. Ionic mobility is directly related to diffusion coefficient, D_j, through the Einstein–Smoluchowski equation [10], Eq. (10).

$$u_j = \frac{z_j F}{RT} D_j \tag{10}$$

Thus, to obtain D_{Cl^-} it is necessary to know u_{Cl^-}, and for this several simplifications are necessary. Firstly, if sample's pores are filled with high concentration NaCl solution, the contribution to conductivity (Eq. (9)) of the intrinsic ions present in mortar's pores (OH^-, Ca^{2+}, K^+...) can be neglected. Typical ionic composition of cement paste filtrate solution is given [11] in Table 5. Although ionic mobility for OH^- is high, the error can be estimate lower than 10% if the filling solution is 1 M NaCl. In this way, the conductivity in mortar samples can be treated as due to 1:1 electrolyte (NaCl). Moreover, the ratio between u_{Na^-} and u_{Cl^-} must be known in order to discriminate both contributions in the total conductivity. The concept of liquid junction potential, ΔE, defined in Eq. (11) can help in this task.

$$\Delta E = (t_+ - t_-)\frac{RT}{F}\ln\frac{a_1}{a_2} \tag{11}$$

In Eq. (11) t_- and t_+ hold for the transport numbers of the anion and the cation, respectively; and a_1 and a_2 for the activities of the 1:1 electrolyte at both sides of the membrane.

Thus, as for 1:1 electrolytes $t_+ + t_- = 1$, the measurement of ΔE in Eq. (11) allows obtaining t_+ and t_-. From these values and Eq. (12) the quantity u_+/u_- can be evaluated.

$$t_+ = \frac{u_+}{u_+ + u_-}, \quad t_- = \frac{u_-}{u_+ + u_-} \tag{12}$$

The liquid junction potential has been measured using a water saturated mortar sample placed between the two-compartments of the permeation cell. The electrolytes in the compartments were 1 M NaCl and 0.1 M NaCl. The measured liquid junction potential at the steady state was 11.6 mV so, the corresponding transport numbers result: $t_+ = 0.39$ and $t_- = 0.61$. Therefore, $u_{Na^+}/u_{Cl^-} = 0.639$, value close to that found for ideal solutions (0.656). $T = 298$ K was employed.

Once the ratio u_{Na^+}/u_{Cl^-} is known, it is possible to directly correlate R_1 and D_{Cl^-} using Eqs. (8)–(10). The resulting equation is given in Eq. (13).

$$D_{Cl^-} = \frac{A}{R_1} \text{ being } A = \frac{R \cdot T \cdot a}{1.639 \cdot F^2 \cdot C_{Cl^-}} \tag{13}$$

Table 5
Typical ionic composition of cement paste filtrate (from reference [11])

Ion	Ca^{2+}	K^+	Na^+	SO_4^{2-}	OH^-
Concentration (mmol L^{-1})	15.38	202.62	55.28	80.79	127.08

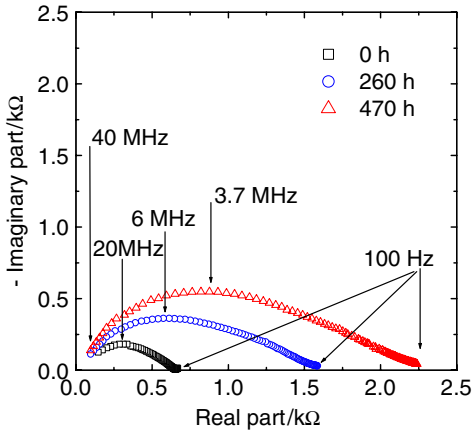

Fig. 13. Evolution of the impedance (Nyquist plot) with testing time for a mortar sample saturated with 1 M NaCl + 0.01 M NaOH. Impedance obtained with two-electrode arrangement.

Diffusion coefficients calculations have been performed using Eq. (13) on mortar samples saturated with solution 1 M NaCl, pH 12. Some of the obtained impedance spectra as a function of time are shown in Fig. 13. The overall impedance follows the general trend already described for migration tests: the impedance increases with time and the apex frequency of the capacitive arc shifts towards lower frequencies.

Fig. 14 summarises the R_1 values obtained from fitting of impedance data to Eq. (7) as well as the corresponding D_{Cl^-} values from Eq. (13). It can be seen in this figure an exponential decay of D_{Cl^-} values with time towards an asymptotic value about 10^{-8} cm^2 s^{-1}, which should correspond to the end of the Friedel's salt formation process and therefore to the achievement of steady-state conditions at about 600 h testing.

The diffusion coefficient data presented in Fig. 14 are fully consistent with those reported in Table 4 as concerning trend and range of absolute value. Thus it can be concluded that the proposed impedance method allows obtaining real time chloride diffusion coefficient values, with the advantage that no DC currents are necessary.

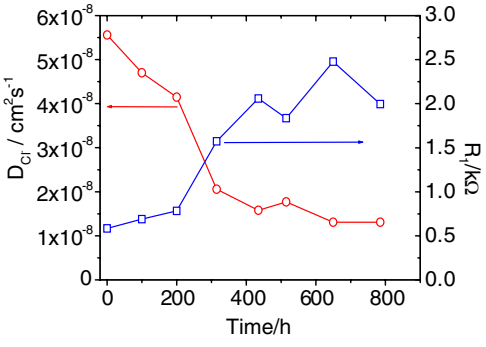

Fig. 14. Evolution with time of R_1 values and diffusion coefficients calculated using Eq. (13). Some of the impedance spectra are given in Fig. 13.

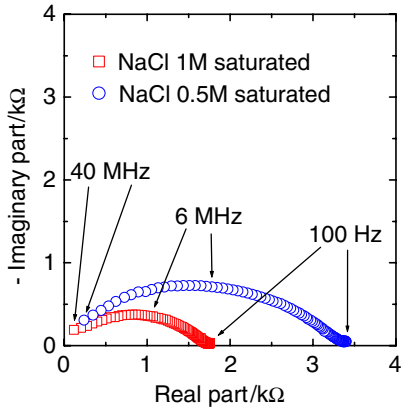

Fig. 15. Comparison of impedance spectra obtained on a mortar sample soaked with NaCl solutions 1 M and 0.5 M.

3.6. Self-consistency of the method

The self-consistency of the method has been checked by changing the concentration of the soaking solution between 1 M NaCl and 0.5 M NaCl. The impedance results appear in Fig. 15 where it can be seen that the overall impedance decreases as electrolyte concentration increases. The relevant parameters obtained from the fitting procedure are $R_e = 609$ and 324 Ω, for the 0.5 M and 1 M solution, respectively. $R_1 = 2722$ and 1290 Ω, also for the diluted and concentrated solution, respectively. It can be seen that R_e scales reasonably well with electrolyte concentration. Moreover, the diffusion coefficients obtained from R_1 are 2.38×10^{-8} cm^2 s^{-1} and 2.51×10^{-8} cm^2 s^{-1}, for the diluted and concentrated solution, respectively. Thus, the measured diffusion coefficient results independent of the electrolyte concentration (see Eq. (13)). The small discrepancies observed can be attributed to the higher relative effect of OH^- in the diluted solution.

4. Conclusions

The proposed impedance method for measuring chloride diffusion coefficients in mortar produces values comparable with those obtained by traditional migration and diffusion techniques.

The proposed method allows obtaining real time information of the variation of diffusion coefficient with time because impedance measurements can be automated.

The method can be applied as stand-alone technique or superimposed to classical migration or diffusion tests.

The full frequency domain impedance spectrum allows obtaining diffusion coefficients and also useful information about sample's microstructure. If only diffusion coefficients are required, a single frequency measurement at about 1 kHz (to overcome interface effects) will be enough, provided that the driven electrodes are close enough to minimise electrolyte resistance.

Acknowledgement

The authors wish to acknowledge the Spanish ''Ministerio de Educación y Ciencia'' for financial support under project MAT2004-06435-C02-01.

References

[1] Hooton RD, Thomas MDA, Stanish K. Testing the chloride penetration resistance of concrete: A literature review, prediction of chloride penetration in concrete, Federal Highway Administration (USA), Publication No. FHWA-RD-00-142 (2000).
[2] Andrade C. Calculation of chloride diffusion coefficients in concrete from ionic migration measurements. Cem Concr Res 1993;23:724–42.
[3] Alonso C, Andrade C, Keddam M, Nóvoa XR, Takenouti H. Impedance measurements on cement paste. Cem Concr Res 1997;27:1191–201.
[4] Alonso C, Andrade C, Nóvoa XR, Keddam M, Takenouti H. Study of the dielectric characteristics of cement paste. Mater Sci Forum 1998;289-292:15–28.
[5] Andrade C, Blanco VM, Collazo A, Keddam M, Nóvoa XR, Takenouti H. Cement paste hardening process studied by impedance spectroscopy. Electrochim Acta 1999;44:4313–8.
[6] Cabeza M, Merino P, Miranda A, Nóvoa XR, Sánchez I. Impedance spectroscopy study of hardened portland cement paste. Cem Concr Res 2002;32:881–91.
[7] Andrade C, Sanjuan MA. Experimental procedure for the calculation of chloride diffusion coefficients in concrete from migration test. Adv Cem Res 1994;6:127–34.
[8] Cabeza M, Keddam M, Nóvoa XR, Sánchez I, Takenouti H. Impedance spectroscopy to characterize the pore structure during the hardening process of portland cement paste. Electrochim Acta 2006;51:1831–41.
[9] Bard AJ, Faulkner LR. Electrochemical methods: fundamentals and applications. second ed. John Wiley and Sons; 2001. p. 65–7.
[10] Bard AJ, Faulkner LR. Electrochemical methods: fundamentals and applications. second ed. John Wiley and Sons; 2001. p. 139.
[11] Carnot A, Frateur I, Marcus P, Tribollet B. Corrosion mechanisms of steel concrete moulds in the presence of a demoulding agent. J. Appl. Electrochem. 2002;32:865–9.